Springer

KSME

Journal of Mechanical Science and Technology 24 (8) (2010) 1743~1752
www.springerlink.com/content/1738-494x
DOI 10.1007/s12206-010-0516-z

# Robust tracking of robot manipulator with nonlinear friction using time delay control with gradient estimator †

Dong Ki Han* and Pyung-hun Chang

*Department of Mechanical Engineering, Korea Advanced Institute of Science and Technology, 373-1, Guseong-dong, Yuseong-gu, Daejeon, Korea*

(Manuscript Received November 9, 2009; Revised March 16, 2010; Accepted May 4, 2010 )

**Abstract**

We propose an enhanced controller to improve the robustness of Time Delay Control (TDC) for a robot manipulator in the presence of nonlinear friction, such as Coulomb friction. The problem of TDC is first analyzed with TDC as a trajectory control for a robot manipulator in the presence of nonlinear friction. Gradient estimation is used to solve this problem. The proposed controller is called TDC with Gradient Estimator (TDCGE). Comparing with a prior research to improve the robustness of TDC, named TDCSA, the TDCGE is much simpler to design. Through 1 DOF linear motor experiment, it is verified that the TDCGE is more robust against nonlinear friction than TDC and the TDCGE has a similar robustness to the TDCSA. In addition, it is confirmed that the TDCGE is easily implemented in the multi degree-of-freedom robot manipulator through a 3 DOF spatial robot manipulator experiment.

*Keywords*: Robust tracking control; Robot manipulator; Time delay control; Nonlinear friction; Gradient estimation

## 1. Introduction

The Time Delay Control (TDC) [1-3] is a control technique which compensates for system uncertainties - for example, unmodeled dynamics, parameter variations and disturbances -by utilizing time delay estimation (TDE) without modeling, and inserts desired dynamics into the plant. Owing to the effectiveness and efficiency of the time delay estimation (TDE), the TDC is robust and yet is characterized by a compact structure and relatively simple gain selection procedure. So, The TDC has been applied to many mechanical systems and control schemes, with consistently good results. [4-9]

However, in the presence of nonlinear friction, TDC shows noticeable performance degradation [10]. Coulomb friction and stiction often cause large tracking errors as a consequence of their rapid dynamics when a plant crosses zero velocity.

Nonlinear friction is not only common in practice but also has significant effects on robot dynamics. Coulomb friction is everywhere and accounts for as much as 30 percent of the maximum motor torque in some robot drive trains, such as a PUMA arm [11]. Static friction is dominant in robot manipulators that incorporate, for example, pneumatic cylinder systems [10] and pneumatic valve [12]; yet, it can occur in any plant although its level is insignificant.

Recently, to overcome the performance degradation of the TDC in the nonlinear friction, the TDC was combined with switching action based on sliding mode control (SMC) [10, 13, 14]. This control scheme was named the TDCSA. The TDCSA was applied to robot manipulators and excavator systems with good results. The TDCSA, however, was associated with some drawbacks. First, the use of signum function tended to cause chattering in the tracking response. In addition, two extra gain matrixes tuning were needed if signum function was replaced with saturation function in order to avoid chattering; these imposed a further burden on the design of the controller.

Accordingly, an enhanced robust control for robot manipulator in the presence of nonlinear friction is proposed in this paper. The proposed control consists of one estimator to overcome the effect of nonlinear friction and an original TDC for robot manipulators. The proposed control is called the TDC with gradient estimator (TDCGE). Gradient estimation is very simple, always convergent and more robust against time-varying parameter than other estimation methods, such as a standard least square estimation. By the gradient estimator, the effect of nonlinear friction is suppressed without modeling and chattering in the tracking response. Moreover, although the gradient estimator has an additional gain matrix, which should be tuned, the selection procedure of this gain matrix is simple

† This paper was recommended for publication in revised form by Associate Editor Jong Hyeon Park
* Corresponding author. Tel.: +82 42 350 3266, Fax.: +82 42 350 2566
E-mail address: dkhan@mecha.kaist.ac.kr

and intuitional. As a result, the TDCGE can be simply implementable than the TDCSA. The property of the gradient estimator is discussed in Section 3. Through 1 DOF linear motor experiment, it is verified that the TDCGE is more robust against nonlinear friction than the TDC and the TDCGE has a similar robustness to the TDCSA. Of course, we confirm that the TDCGE is much more implementable than the TDCSA. In addition, through 3 DOF spatial robot manipulator experiment, we also confirm that the TDCGE is easily implemented in the multi degree-of-freedom robot manipulator.

This paper is outlined as follows. In Section 2, the TDC are briefly reviewed and its problem is analyzed. The enhanced robust controller is proposed and some of its properties are analyzed in Section 3. The practical design procedure of the proposed control is also discussed in Section 3. In Section 4, the advantages of the TDCGE are verified through a 1 DOF linear motor and a 3 DOF spatial robot manipulator experiment. At last, concluding remarks are given in Section 5.

## 2. Problems of TDC due to the TDE error

We summarize the Time Delay Control (TDC) scheme for robot manipulators [4] and analyze its problems concerning the TDE error [10].

### *2.1 Review of the TDC*

The dynamics Eq. of a n DOF robot manipulator in joint space coordinates is given by:

$$\boldsymbol{\tau} = \mathbf{M}(\boldsymbol{\theta})\ddot{\boldsymbol{\theta}} + \mathbf{V}(\boldsymbol{\theta},\dot{\boldsymbol{\theta}}) + \mathbf{G}(\boldsymbol{\theta}) + \mathbf{F} + \mathbf{D}\,, \tag{1}$$

where $\boldsymbol{\tau} \in \Re^n$ denotes the actuator torque; $\boldsymbol{\theta},\dot{\boldsymbol{\theta}},\ddot{\boldsymbol{\theta}} \in \Re^n$ the joint angle, joint angular velocity, and joint angular acceleration, respectively; $\mathbf{M}(\boldsymbol{\theta}) \in \Re^{n\times n}$ the inertia matrix; $\mathbf{V}(\boldsymbol{\theta},\dot{\boldsymbol{\theta}}) \in \Re^n$ the Coriolis and the centrifugal forces; $\mathbf{G}(\boldsymbol{\theta}) \in \Re^n$ terms due to gravity; $\mathbf{F},\mathbf{D} \in \Re^n$ friction term and disturbance, respectively. Introducing a constant matrix $\bar{\mathbf{M}}$, another expression of (1) is obtained as follows:

$$\boldsymbol{\tau} = \bar{\mathbf{M}}\ddot{\boldsymbol{\theta}} + \mathbf{H}(\boldsymbol{\theta},\dot{\boldsymbol{\theta}},\ddot{\boldsymbol{\theta}})\,, \tag{2}$$

where $\bar{\mathbf{M}} \in \Re^{n\times n}$ is positive definite diagonal matrix; $\mathbf{H}(\boldsymbol{\theta},\dot{\boldsymbol{\theta}},\ddot{\boldsymbol{\theta}})$ the total sum of the nonlinear dynamics of robot manipulators, frictions and disturbances and is described as:

$$\begin{aligned}\mathbf{H}(\boldsymbol{\theta},\dot{\boldsymbol{\theta}},\ddot{\boldsymbol{\theta}}) = &\left[\mathbf{M}(\boldsymbol{\theta}) - \bar{\mathbf{M}}\right]\ddot{\boldsymbol{\theta}} + \mathbf{V}(\boldsymbol{\theta},\dot{\boldsymbol{\theta}}) \\ &+ \mathbf{G}(\boldsymbol{\theta}) + \mathbf{F} + \mathbf{D}\end{aligned}\,. \tag{3}$$

The control objective of TDC, like the computed torque method is to achieve the following error dynamics as follows:

$$\ddot{\mathbf{e}} + \mathbf{K_D}\dot{\mathbf{e}} + \mathbf{K_P}\mathbf{e} = \mathbf{0}\,, \tag{4}$$

where $\mathbf{e} \triangleq \boldsymbol{\theta}_\mathbf{d} - \boldsymbol{\theta}$ denotes a tracking error vector. To this end,

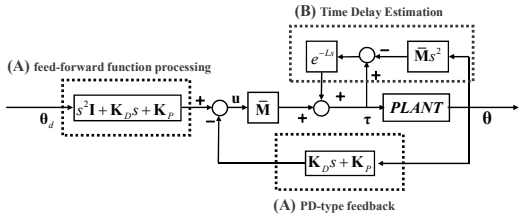


Fig. 1. Block diagram of the TDC: dashed box (A) denotes the part to inject desired error dynamics; (B) Time Delay Estimation (TDE).

the computed torque $\boldsymbol{\tau}$ is designed based on the computed torque control as follows:

$$\boldsymbol{\tau} = \bar{\mathbf{M}}\mathbf{u} + \hat{\mathbf{H}}(\boldsymbol{\theta},\dot{\boldsymbol{\theta}},\ddot{\boldsymbol{\theta}})\,, \text{ and} \tag{5}$$

$$\mathbf{u} = \ddot{\boldsymbol{\theta}}_\mathbf{d} + \mathbf{K_D}(\dot{\boldsymbol{\theta}}_\mathbf{d} - \dot{\boldsymbol{\theta}}) + \mathbf{K_P}(\boldsymbol{\theta}_\mathbf{d} - \boldsymbol{\theta})\,, \tag{6}$$

where $\hat{\mathbf{H}}(\boldsymbol{\theta},\dot{\boldsymbol{\theta}},\ddot{\boldsymbol{\theta}})$ denotes the estimated value of $\mathbf{H}(\boldsymbol{\theta},\dot{\boldsymbol{\theta}},\ddot{\boldsymbol{\theta}})$; $\boldsymbol{\theta}_\mathbf{d},\dot{\boldsymbol{\theta}}_\mathbf{d},\ddot{\boldsymbol{\theta}}_\mathbf{d} \in \Re^n$ desired position, desired velocity, and desired acceleration, respectively; and $\mathbf{K_D} \in \Re^{n\times n}$, $\mathbf{K_P} \in \Re^{n\times n}$ represent the diagonal gain matrices of decoupled PD controllers. In essence, the control (5) attempts to cancel $\mathbf{H}(\boldsymbol{\theta},\dot{\boldsymbol{\theta}},\ddot{\boldsymbol{\theta}})$ in (2) by $\hat{\mathbf{H}}(\boldsymbol{\theta},\dot{\boldsymbol{\theta}},\ddot{\boldsymbol{\theta}})$ and inject a desired dynamics in (6). Whereas the computed torque method incorporates real-time computation of $\hat{\mathbf{H}}(\boldsymbol{\theta},\dot{\boldsymbol{\theta}},\ddot{\boldsymbol{\theta}})$ based on a robot dynamic model, TDC uses the time delay estimation (TDE) described as follows:

$$\mathbf{H}(\boldsymbol{\theta},\dot{\boldsymbol{\theta}},\ddot{\boldsymbol{\theta}}) \approx \mathbf{H}(\boldsymbol{\theta},\dot{\boldsymbol{\theta}},\ddot{\boldsymbol{\theta}})_{t-L} \triangleq \hat{\mathbf{H}}(\boldsymbol{\theta},\dot{\boldsymbol{\theta}},\ddot{\boldsymbol{\theta}})\,, \tag{7}$$

which is the essential idea of the TDC. Notice that $\bullet_{t-L}$ means time delayed valued of $\bullet$. Under the assumption that $\mathbf{H}$ is continuous or piecewise continuous and the time delay $L$ is sufficiently small, the TDE is the excellent estimation of $\mathbf{H}$.

The TDE can be derived from (2) as follows:

$$\mathbf{H}(\boldsymbol{\theta},\dot{\boldsymbol{\theta}},\ddot{\boldsymbol{\theta}})_{t-L} = \boldsymbol{\tau}_{t-L} - \bar{\mathbf{M}}\ddot{\boldsymbol{\theta}}_{t-L}\,. \tag{8}$$

Note that (8) is a causal relationship. The final form of TDC results from (5)-(8) like this:

$$\begin{aligned}\boldsymbol{\tau} = &\underbrace{\boldsymbol{\tau}_{t-L} - \bar{\mathbf{M}}\ddot{\boldsymbol{\theta}}_{t-L}}_{\mathbf{TDE}\text{ : to cancel out }\mathbf{H}(\boldsymbol{\theta},\dot{\boldsymbol{\theta}},\ddot{\boldsymbol{\theta}})} \\ &+\bar{\mathbf{M}}\underbrace{\left[\ddot{\boldsymbol{\theta}}_\mathbf{d} + \mathbf{K_D}(\dot{\boldsymbol{\theta}}_d - \dot{\boldsymbol{\theta}}) + \mathbf{K_P}(\boldsymbol{\theta}_\mathbf{d} - \boldsymbol{\theta})\right]}_{\mathbf{u}\text{: to inject desired error dynamics}}\end{aligned}\,. \tag{9}$$

Owing to the TDE, the TDC has a simple structure and is very efficient – approximately as efficient as a typical PID control. Furthermore, since $\bar{\mathbf{M}}$ is selected as a diagonal matrix, the TDC can be designed for n individual joint controllers by using each diagonal element of $\bar{\mathbf{M}}$, that of $\mathbf{K_D}$, and that of $\mathbf{K_P}$. Fig. 1 shows the block diagram of the closed-loop system due to the TDC. Notice that the TDC may be viewed as consisting of two functions: (A) $\mathbf{u}$ to inject desired error dynamics (feed-forward function processing $\boldsymbol{\theta}_d$ + PD-type

feedback of $\boldsymbol{\theta}$ ); (B) TDE to cancel out $\mathbf{H}\left(\boldsymbol{\theta},\dot{\boldsymbol{\theta}},\ddot{\boldsymbol{\theta}}\right)$.

### *2.2 Problems of the TDC concerned with the TDE error*

If the time delay $L$ is set infinitesimally small, a perfect estimation of $\mathbf{H}\left(\boldsymbol{\theta},\dot{\boldsymbol{\theta}},\ddot{\boldsymbol{\theta}}\right)$ would be possible by using the TDE. Because of digital implementation, however, the smallest value for the time delay $L$ is the sampling time, which is finite. Therefore, the estimation error results from a finite $L$. The following relationship is derived from substituting (5) into (2) and considering (7):

$$\begin{aligned}&\mathbf{H}\left(\boldsymbol{\theta},\dot{\boldsymbol{\theta}},\ddot{\boldsymbol{\theta}}\right)-\hat{\mathbf{H}}\left(\boldsymbol{\theta},\dot{\boldsymbol{\theta}},\ddot{\boldsymbol{\theta}}\right)\\&=\mathbf{H}\left(\boldsymbol{\theta},\dot{\boldsymbol{\theta}},\ddot{\boldsymbol{\theta}}\right)-\mathbf{H}\left(\boldsymbol{\theta},\dot{\boldsymbol{\theta}},\ddot{\boldsymbol{\theta}}\right)_{t-L}=\bar{\mathbf{M}}\left(\mathbf{u}-\ddot{\boldsymbol{\theta}}\right)\end{aligned}. \tag{10}$$

The LHS of the above Eq. denotes the estimation error. Now define the TDE error, $\boldsymbol{\varepsilon}$ as follows:

$$\boldsymbol{\varepsilon}\triangleq\bar{\mathbf{M}}^{-1}\left[\mathbf{H}\left(\boldsymbol{\theta},\dot{\boldsymbol{\theta}},\ddot{\boldsymbol{\theta}}\right)-\mathbf{H}\left(\boldsymbol{\theta},\dot{\boldsymbol{\theta}},\ddot{\boldsymbol{\theta}}\right)_{t-L}\right]=\mathbf{u}-\ddot{\boldsymbol{\theta}}\,. \tag{11}$$

Substituting (6) into (11), we obtain the closed-loop error dynamics of TDC as follows:

$$\boldsymbol{\varepsilon}=\ddot{\mathbf{e}}+\mathbf{K_D}\dot{\mathbf{e}}+\mathbf{K_P}\mathbf{e}\,. \tag{12}$$

Eq. (12) clearly shows the impact of the TDE error, $\boldsymbol{\varepsilon}$ on the desired error dynamics: $\boldsymbol{\varepsilon}$ causes the resulting dynamics to deviate from the desired error dynamics.

Especially, under nonlinear frictions, such as Coulomb friction and static friction, $\mathbf{F}$ of (3) becomes discontinuous and then the continuity assumption of $\mathbf{H}\left(\boldsymbol{\theta},\dot{\boldsymbol{\theta}},\ddot{\boldsymbol{\theta}}\right)$ in (7) is invalid. As a result, a large TDE error is occurred in (11) under nonlinear frictions. A large TDE error results in a large tracking error as (12).

## 3. Proposition: Time Delay Control with Gradient Estimator (TDCGE)

An enhanced controller, which has a function to compensate for the TDE error, is proposed. The proposed control is called Time Delay Control with Gradient Estimator (TDCGE). The gradient estimator of the TDCGE estimates and compensates for the TDE error. The properties of the gradient estimator are analyzed in detail. For real implementation of the TDCGE, practical design procedure of the TDCGE is also introduced.

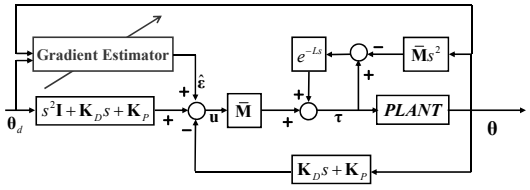


Fig. 2. The block diagram of the TDCGE: original TDC + Gradient Estimator.

### *3.1 Derivation of the TDCGE*

To estimate and compensate for the TDE error, the gradient estimator term, $\hat{\boldsymbol{\varepsilon}}$ is introduced in the control input of the TDC(9). Combining previous formulation, the control law of the TDCGE is proposed by

$$\begin{aligned}\boldsymbol{\tau}=\;&\underbrace{\boldsymbol{\tau}_{t-L}-\bar{\mathbf{M}}\ddot{\boldsymbol{\theta}}_{t-L}}_{\textbf{T}\text{ime }\textbf{D}\text{elay }\textbf{E}\text{stimation}}\\&+\underbrace{\bar{\mathbf{M}}\left[\ddot{\boldsymbol{\theta}}_{\mathbf{d}}+\mathbf{K_D}\left(\dot{\boldsymbol{\theta}}_d-\dot{\boldsymbol{\theta}}\right)+\mathbf{K_P}\left(\boldsymbol{\theta}_{\mathbf{d}}-\boldsymbol{\theta}\right)\right]}_{\mathbf{u}\text{: to inject desired error dynamics}}\\&+\underbrace{\bar{\mathbf{M}}\hat{\boldsymbol{\varepsilon}}}_{\textbf{Gradient Estimator}\text{: to compensate for TDE error}}\end{aligned}. \tag{13}$$

Then, with the combination of (13) and (2), the closed-loop error dynamics of the TDCGE is defined as follows:

$$\ddot{\mathbf{e}}+\mathbf{K_D}\dot{\mathbf{e}}+\mathbf{K_P}\mathbf{e}=\boldsymbol{\varepsilon}-\hat{\boldsymbol{\varepsilon}}=-\tilde{\boldsymbol{\varepsilon}}\,, \tag{14}$$

where $\tilde{\boldsymbol{\varepsilon}}\triangleq\hat{\boldsymbol{\varepsilon}}-\boldsymbol{\varepsilon}$ denotes the estimation error about the TDE error.

A cost function of the estimation error was made as follows:

$$\mathbf{J}\left(\tilde{\boldsymbol{\varepsilon}}\right)=\frac{1}{2}\tilde{\boldsymbol{\varepsilon}}^{\mathrm{T}}\tilde{\boldsymbol{\varepsilon}}\,. \tag{15}$$

If the TDE error was slow-varying or constant, the gradient estimator was designed by the gradient method as follows:

$$\dot{\hat{\boldsymbol{\varepsilon}}}=-\mathbf{K_{GE}}\frac{\partial\mathbf{J}}{\partial\hat{\boldsymbol{\varepsilon}}}=-\mathbf{K_{GE}}\tilde{\boldsymbol{\varepsilon}}=\mathbf{K_{GE}}\left(\ddot{\mathbf{e}}+\mathbf{K_D}\dot{\mathbf{e}}+\mathbf{K_P}\mathbf{e}\right), \tag{16}$$

where $\mathbf{K_{GE}}\triangleq diag\left(K_{GE_1},\ldots,K_{GE_n}\right)$ denotes the estimator gain matrix of which elements are always positive. The gradient estimator in (16) is updated in the direction of decreasing TDE error, because the gradient estimator always makes the slope of cost function be negative.

The overall control law of the TDCGE is as follows:

$$\begin{aligned}\boldsymbol{\tau}=\;&\underbrace{\boldsymbol{\tau}_{t-L}-\bar{\mathbf{M}}\ddot{\boldsymbol{\theta}}_{t-L}}_{\textbf{T}\text{ime }\textbf{D}\text{elay }\textbf{E}\text{stimation}}\\&+\underbrace{\bar{\mathbf{M}}\left[\ddot{\boldsymbol{\theta}}_{\mathbf{d}}+\mathbf{K_D}\left(\dot{\boldsymbol{\theta}}_d-\dot{\boldsymbol{\theta}}\right)+\mathbf{K_P}\left(\boldsymbol{\theta}_{\mathbf{d}}-\boldsymbol{\theta}\right)\right]}_{\mathbf{u}\text{: to inject desired error dynamics}},\\&+\underbrace{\bar{\mathbf{M}}\hat{\boldsymbol{\varepsilon}}}_{\textbf{Gradient Estimator}\text{: to compensate for TDE error}}\end{aligned} \tag{17}$$

where

$$\hat{\boldsymbol{\varepsilon}}=\mathbf{K_{GE}}\left(\dot{\mathbf{e}}+\mathbf{K_D}\mathbf{e}+\mathbf{K_P}\int\mathbf{e}dt\right). \tag{18}$$

The block diagram of the TDCGE is shown in Fig. 2. Notice that the TDCGE only consists of an original TDC for a robot manipulator [4] and the gradient estimator. Because of

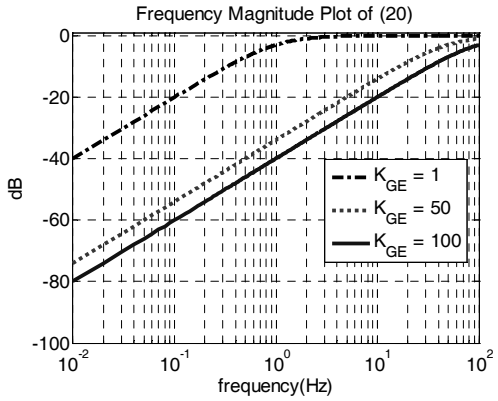


Fig. 3. Frequency magnitude plot of (20).

using the TDE, the TDCGE does not need a complete computation of the robot dynamics as the TDC. The additional integral term in (18), $\mathbf{K_{GE}K_P}\int \mathbf{e}dt$ makes the TDCGE have better control performance than the TDC.

Note that the TDCGE has only one additional gain matrix $\mathbf{K_{GE}}$, whereas the TDCSA has two extra gain matrixes. As a result, the TDCGE can be simply implementable than the TDCSA.

The stability analysis of the TDCGE is analyzed in Appendix.

### *3.2 Gradient estimator: High-pass filter for the TDE error*

In order simply to analyze the property of the gradient estimator, assume that we apply the TDCGE to 1 DOF robot manipulator.

From $\tilde{\varepsilon} \triangleq \hat{\varepsilon} - \varepsilon$ and (16), the time derivative of the estimation error about TDE error $\tilde{\varepsilon}$ can be obtained as:

$$\dot{\tilde{\varepsilon}} = \dot{\hat{\varepsilon}} - \dot{\varepsilon} = -K_{GE} \cdot \tilde{\varepsilon} - \dot{\varepsilon}\,, \tag{19}$$

where $\varepsilon$ denotes the TDE error as (12); $\hat{\varepsilon}$ the gradient estimator term of the TDCGE (13).

The frequency response function of (19) is derived as follows:

$$\left|G(j\omega)\right| = \left|\frac{\tilde{\varepsilon}(j\omega)}{\varepsilon(j\omega)}\right| = \frac{\omega(1/K_{GE})}{\sqrt{1+\left[\omega(1/K_{GE})\right]^2}}\,. \tag{20}$$

Fig. 3 shows the frequency magnitude plot of (20). Fig. 3 shows that the low frequency part of the TDE error $\varepsilon(s)$ is cancelled out by the gradient estimator. Therefore, the gradient estimator can be thought as a high-pass filter for the TDE error. The cut-off frequency of this filter is $K_{GE}$. As increasing $K_{GE}$, the better robustness against the TDE error is expected in the TDEGE. However, the very large $K_{GE}$ cannot be used in the real implementation of the TDCGE. The detailed selection procedure of $K_{GE}$ is demonstrated later.

Through the simulation using 1 DOF manipulator (Fig. 4)

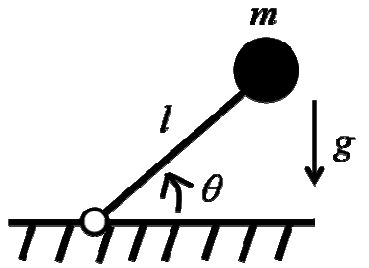


Fig. 4. 1 DOF manipulator: $m = 1.0(\mathrm{kg})$ and $l = 1.0(\mathrm{m})$.

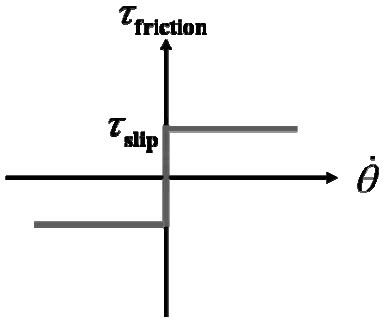


Fig. 5. Coulomb friction model: $\tau_{slip} = 5.0(\mathrm{Nm})$ denotes the Coulomb friction coefficient.

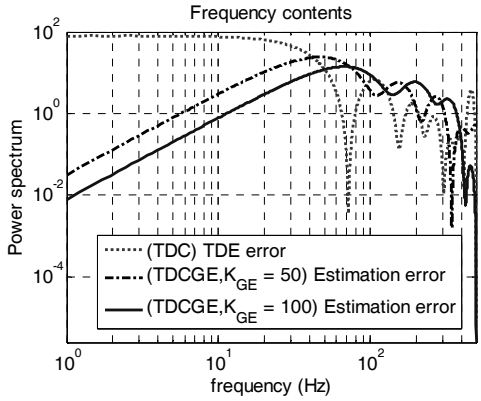


Fig. 6. Frequency Contents of TDE error, $\varepsilon$ and the Estimation error about TDE error, $\tilde{\varepsilon}$.

with Coulomb friction model (Fig. 5), one of nonlinear friction, it is verified whether the low frequency part of the TDE error is compensated by the gradient estimator or not. Notice that the control gains of the TDC and the TDCGE in this simulation are determined as $\bar{M} = 1.0$, $K_D = 20$, $K_P = 100$ and $L = 0.001\mathrm{sec}$. And the estimator gain of the gradient estimator in TDCGE is chosen as $K_{GE} = 50$ or $100$. The desired trajectory of this simulation is set as follows:

$$\theta_{d1}(t) = 10.0\sin\left(\frac{\pi}{2}t\right)(\mathrm{deg})\,. \tag{21}$$

Fig. 6 shows the power spectrum of the TDE error, defined as(12) in the case of TDC and the power spectrum of the estimation error about the TDE error, defined as (14) in the case

of TDCGE. Through Fig. 6, we confirm that the gradient estimator compensates for the low frequency part of the TDE error and the low frequency part of the TDE error is more cancelled out with an increase in $K_{GE}$.

Notice that, in the design of the gradient estimator, we used one assumption as follows: the TDE error was slow-varying or constant. Through Eq. (19) and (20), it is confirmed that the gradient estimator sufficiently compensates for the low frequency part of the TDE error under the situation that the TDE error is not constant or slow-varying.

### *3.3 Practical design procedure of the TDCGE*

The proposed control has quite a few design variables; one can design the controller only by choosing the gains ($\bar{\mathbf{M}}$, $\mathbf{K_D}$, $\mathbf{K_P}$ and $\mathbf{K_{GE}}$) and the sampling time $L$. It is another advantage of the TDCGE that the choice of the gains ($\bar{\mathbf{M}}$, $\mathbf{K_D}$, $\mathbf{K_P}$ and $\mathbf{K_{GE}}$) and the sampling time $L$ are as simple as the TDC. Especially only two gain matrices, $\bar{\mathbf{M}}$ and $\mathbf{K_{GE}}$ must be tuned for control law. The design procedure of the TDCGE is introduced briefly in the following.

**Step 1: Select a sampling time interval $L$**

Select a sampling time interval $L$ of closed-loop system with considering the speed of the controller hardware [15]. Commonly, faster sampling provides better performance because smaller $L$ makes the TDE in (7) more exact.

**Step 2: Determine desired error dynamics**

Determine desired error dynamics in (4) for each joint. After choosing the desired natural frequency, $\omega_{ni}$, and the desired damping ratio, $\varsigma_i$, one can systematically design $\mathbf{K_D}$ and $\mathbf{K_P}$ whose diagonal elements are $K_{Di} = 2\varsigma_i\omega_{ni}$ and $K_{Pi} = \omega_{ni}^{\ 2}$, respectively.

**Step 3: Gain tuning of $\bar{\mathbf{M}}$**

The best performance was obtained by directly using the diagonal elements of $\mathbf{M}(\boldsymbol{\theta})$ directly in the simulation without noise. For real system, the tuning of $\bar{\mathbf{M}} = diag(\alpha_1,\cdots,\alpha_n)$ is dependent on the diagonal elements of $\mathbf{M}(\boldsymbol{\theta})$ and the noise of the system as below. The effect of the noise may be amplified due to calculation of $\ddot{\boldsymbol{\theta}}_{t-L}$ by numerical differentiation introduced in [3]. Fortunately, $\bar{\mathbf{M}}$ of the proposed control has an implicit function of the low pass filter (the same goes for TDC). In detail, it is possible to attenuate noise without explicitly using an additional low-pass filter by lowering $\bar{\mathbf{M}}$ [2].

A simpler formulation of (17) is

$$\begin{aligned}&\boldsymbol{\tau} = \boldsymbol{\tau}_{t-L} + \bar{\mathbf{M}}\left(\mathbf{v} - \ddot{\boldsymbol{\theta}}_{t-L}\right),\\ &\text{where } \mathbf{v} = \ddot{\boldsymbol{\theta}}_{\mathbf{d}} + \mathbf{K_D}\left(\dot{\boldsymbol{\theta}}_d - \dot{\boldsymbol{\theta}}\right) + \mathbf{K_P}\left(\boldsymbol{\theta}_{\mathbf{d}} - \boldsymbol{\theta}\right) + \hat{\boldsymbol{\varepsilon}}\end{aligned} \tag{22}$$

If a digital low-pass filter with the cutoff frequency $\lambda$ is adopted, the control law can be modified as follows:

$$\begin{aligned}\boldsymbol{\tau}^{\text{filtered}} &= \lambda'(1+\lambda')^{-1}\boldsymbol{\tau}\\ &\quad + (1+\lambda')^{-1}\boldsymbol{\tau}_{t-L}^{\text{filtered}} \quad (\lambda' = \lambda L)\end{aligned}, \tag{23}$$

where $\boldsymbol{\tau}$ denotes the input to the filter and $\boldsymbol{\tau}^{\text{filtered}}$ is the output from the filter.

Substituting (22) into (23), the following filtered control law is obtained by

$$\boldsymbol{\tau}^{\text{filtered}} = \boldsymbol{\tau}_{t-L}^{\text{filtered}} + \lambda'(1+\lambda')^{-1}\bar{\mathbf{M}}\left(\mathbf{v} - \ddot{\boldsymbol{\theta}}_{t-L}\right). \tag{24}$$

Comparing (22) and (24) clearly shows that lowering $\bar{\mathbf{M}}$ has the same effect as using a first-order low-pass filter.

Therefore, the detailed gain tuning of $\bar{\mathbf{M}}$ is as follows: After letting $\bar{\mathbf{M}} = diag(\alpha_1,\cdots,\alpha_n)$, one can tune the parameters $\alpha_1$ (for joint 1) to $\alpha_n$ (for joint $n$), separately. For each $\alpha_i$, set $\alpha_i$ as a small positive value at first, then increase $\alpha_i$ just before the closed-loop system has noisy response. After choosing all of $\alpha_i$ for each joint, test the case when all joints are controlled simultaneously; and adjust each $\alpha_i$.

**Step 4: Gain tuning of $\mathbf{K_{GE}}$**

Incidentally, when $\bar{\mathbf{M}}$ is lowered for practical use to filter the noise, the TDE error estimation effect of the last term in (17) would be reduced. In this case, one can increase $\mathbf{K_{GE}}$ as much as possible to make the last term in (17) function effectively. The enhancement of performance is expected as increasing $\mathbf{K_{GE}}$, because the low frequency part of TDE error is more cancelled out with an increase in $\mathbf{K_{GE}}$ as shown in Fig. 6. Notice that the noisy response of closed-loop system can be occurred in a larger $\mathbf{K_{GE}}$, because the high frequency part of estimation error $\tilde{\boldsymbol{\varepsilon}}$ is more dominant as increasing $\mathbf{K_{GE}}$ (Fig. 6). Therefore, the detailed gain tuning of $\mathbf{K_{GE}}$ is as follows: After letting $\mathbf{K_{GE}} = diag\left(K_{GE_1},\ldots,K_{GE_n}\right)$, one can tune the parameters $K_{GE_1}$ (for joint 1) to $K_{GE_n}$ (for joint $n$), separately. For each $K_{GE_i}$, set $K_{GE_i}$ as a small positive value at first, then increase $K_{GE_i}$. The elements of $\mathbf{K_{GE}}$, $K_{GE_i}$ are set with highest possible values without control chatter.

To summarize Section 3, we have derived the TDCGE for robot manipulators in order simply to compensate for TDE error. We have made out that the gradient estimator of the TDCGE can be thought as a high-pass filter for the TDE error. And we have confirmed that the TDCGE has a simple gain selection procedure as the TDC.

## 4. Experimental verification

Through 1 DOF linear motor experiment, it is verified that the TDCGE is more robust against nonlinear friction than TDC and the TDCGE has a similar robustness to the TDCSA. Of course, it is ascertained that the TDCGE is more simply implementable than the TDCSA. In addition, through 3 DOF spatial robot manipulator experiment, it is confirmed that the TDCGE is easily implemented in the multi degree-of-freedom

robot manipulator.

### *4.1 1DOF linear motor experiment*

#### *4.1.1 Experiment setup*

We have experimented on the linear motor, JTM10 shown in Fig. 7. The reduced mathematical model of linear motor system is as follows:

$$\frac{MR_i}{K_T}\frac{d^2x}{dt^2}+K_E\frac{dx}{dt}+\frac{R_i}{K_T}F_f=u, \tag{25}$$

where $x$ denotes the position of motor; $u$ the input voltage; $M=3kg$ the mover mass of motor; $K_T=16N/A$ the force constant; $F_f$ the friction force; $R_i=15.2\Omega$ the electrical resistance; $K_E=16V\cdot\sec/m$ means the back-EMF constant.

The desired trajectory is:

$$x_{d(t)}=10.0\left(1-e^{-\omega_d t}\right)\sin\left(\omega_d t\right)(mm)\,, \tag{26}$$

where $\omega_d$ denotes the frequency of reference trajectory, 0.25Hz.

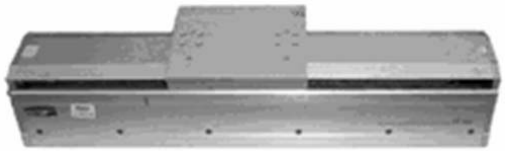

Fig. 7. Linear motor (JTM 10).

The TDC [4] is designed as follows:

$$\begin{aligned}u_{(t)}&=u_{(t-L)}-\bar{M}\ddot{x}_{(t-L)}\\&\quad+\bar{M}\left(\ddot{x}_d+K_D\left(\dot{x}_d-\dot{x}\right)+K_P\left(x_d-x\right)\right)\end{aligned}. \tag{27}$$

The TDCSA [10] is designed as follows:

$$\begin{aligned}u_{(t)}&=u_{(t-L)}-\bar{M}\ddot{x}_{(t-L)}\\&\quad+\bar{M}\left(\ddot{x}_d+K_D\left(\dot{x}_d-\dot{x}\right)+K_P\left(x_d-x\right)\right),\\&\quad+K_{SA}\mathrm{sat}(s,\phi)\end{aligned} \tag{28}$$

where

$$\mathrm{sat}(s_i,\phi_i)=\begin{cases}\dfrac{s_i}{\phi_i} & \text{if } |s_i|<\phi_i\\ \mathrm{sgn}\left(s_i\right) & \text{if } |s_i|\geq\phi_i\end{cases}. \tag{29}$$

And the TDCGE (17) and (18) is designed as follows:

$$\begin{aligned}u_{(t)}&=u_{(t-L)}-\bar{M}\ddot{x}_{(t-L)}\\&\quad+\bar{M}\left(\ddot{x}_d+K_D\left(\dot{x}_d-\dot{x}\right)+K_P\left(x_d-x\right)\right),\\&\quad+\bar{M}\hat{\varepsilon}_{(t)}\end{aligned} \tag{30}$$

where

$$\dot{\hat{\varepsilon}}_{(t)}=K_{GE}\left(\left(\ddot{x}_d-\ddot{x}\right)+K_D\left(\dot{x}_d-\dot{x}\right)+K_P\left(x_d-x\right)\right). \tag{31}$$

Incidentally, the derivative terms, $\dot{x}$ and $\ddot{x}$, are calculated by using numerical differentiation [3].

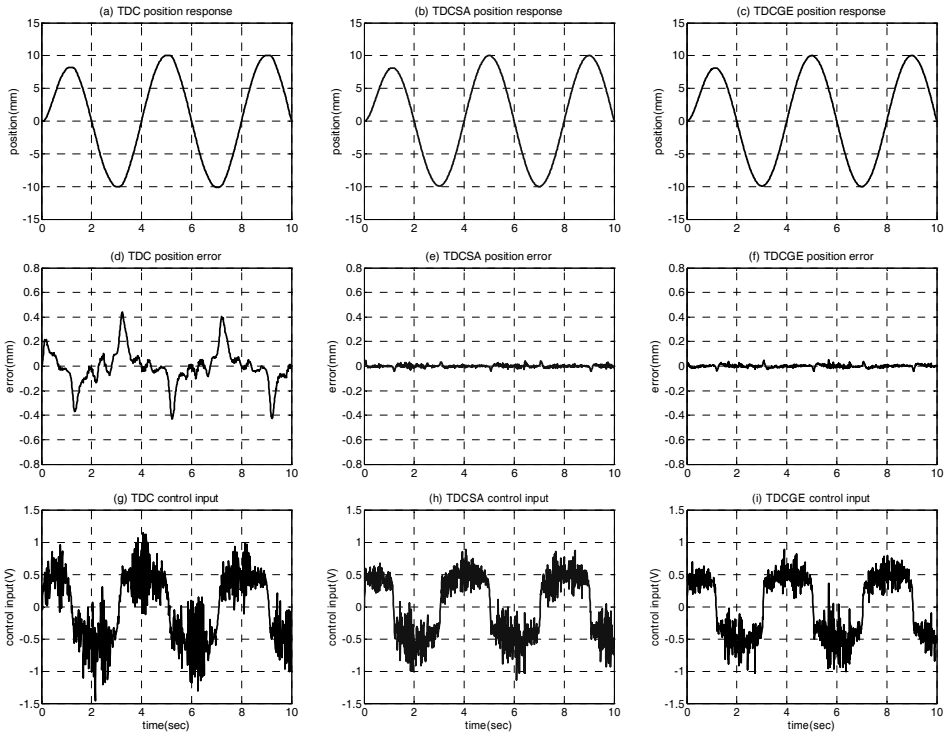


Fig. 8. Experimental Results of Linear Motor - TDC, TDCSA and TDCGE.

Table 1. Control gains for 1 DOF linear motor experiment.

| | TDC | TDCSA | TDCGE |
|---|---|---|---|
| $\bar{M}$ | 0.0003 | 0.0003 | 0.0003 |
| $K_{SA}$ | × | 0.10 | × |
| $\phi$ | × | 7 | × |
| $K_{GE}$ | × | × | 0.0004 |

Table 2. Maximum tracking errors.

| | Maximum tracking errors |
|---|---|
| TDC | ±0.60mm |
| TDCSA | ±0.045mm |
| TDCGE | ±0.048mm |

For the TDC, the TDCSA and the TDCGE, the desired error dynamics in (4) is designed to have same natural frequency and damping ratio as $\omega_n = 10$ rad/s and $\varsigma = 1$ for critical damping, respectively, resulting PD gains $K_D = 20$ and $K_P = 100$. Both the sampling time and the time delay for TDE are set to $L = 0.001$s.

All tuning gains of the TDC, the TDCSA and the TDCGE are best tuned to minimize tracking error as shown in Table 1. Notice that, in the design of the TDCSA, since there is no guide-line to tune $K_{SA}$ and $\phi$, it was very difficult to select them. As a result, we spent much longer time in designing the TDCSA than the TDC or the TDCGE.

#### *4.1.2 Experiment result*

Experimental results are shown in Fig. 8. And maximum tracking errors are arranged in Table 2. The plant controlled by TDC has large tracking error due to coulomb friction, one of nonlinear friction, when the plant passes by zero velocity (Fig. 8(d)). In the TDCGE case, tracking error is substantially reduced, and then it is confirmed that the gradient estimator works well (Fig. 8(f)). The performance of the TDCGE is similar to the case of the TDCSA. As a result, it is ascertained that the TDCGE is more simply implementable control scheme than the TDCSA with an excellent robustness as the TDCSA.

### *4.2 3 DOF spatial robot experiment*

#### *4.2.1 Experiment setup*

We have experimented on a 3 DOF spatial industrial robot, Samsung Faraman-AT2 shown in Fig. 9. Its maximum payload is 3 kg, and the maximum continuous torques are 0.637, 0.637 and 0.319 Nm for joints 1, 2 and 3 respectively. The gear-reduction ration and the encoder resolution of each joint are 120:1 and 2048 pulses/rev, respectively. Resolution of each robot joint is $3.66\times10^{-4}$ deg (quadrature encoder). The parameters of robot dynamics were assumed to be unknown, and thus were not used.

The desired trajectories for all joints are set as follows:

$$\theta_{di} = A_d\left(1-e^{-\omega_d t}\right)\sin\left(\omega_d t\right), \tag{32}$$

Table 3. Maximum tracking error: $e_{\max} = \max\left|e(t)\right|$.

| | (1) TDC | (2) TDCGE | (2)/(1)*100 |
|---|---|---|---|
| Joint1 | 0.0182 deg | 0.0033 deg | 18.13% |
| Joint2 | 0.0313 deg | 0.0111 deg | 35.46% |
| Joint3 | 0.0556 deg | 0.0197 deg | 35.43% |

Table 4. Mean deviations of tracking error: $e_{mean} = \left(t_f - t_0\right)^{-1}\int_{t_0}^{t_f}\left|e(t)\right|dt$

| | (1) TDC | (2) TDCGE | (2)/(1)*100 |
|---|---|---|---|
| Joint 1 | 0.0025 deg | 0.0010 deg | 40.00% |
| Joint 2 | 0.0078 deg | 0.0018 deg | 23.08% |
| Joint 3 | 0.0103 deg | 0.0023 deg | 22.33% |

Fig. 9. 3 DOF spatial robot system.

where $A_d = 10\,\text{deg}$ and $\omega_d = 0.4\pi$ rad/s.

For the TDC (9) and the TDCGE (17), the desired error dynamics in (4) is designed to have same natural frequencies and damping ratios as $\omega_{ni} = 10\,\text{rad/s}$ and $\varsigma_i = 1$, respectively, resulting PD gains $k_{Di} = 20$ and $k_{Pi} = 100$, where $i$ denotes $i$-th joint. The time delay is set with the sampling time, as $L = 0.001$s.

For the TDC and the TDCGE, $\bar{\mathbf{M}}$ was selected by the gain tuning procedure in the Step 3 of Section 3.3, which is

$$\bar{\mathbf{M}} = \begin{bmatrix} 0.031 & 0 & 0 \\ 0 & 0.024 & 0 \\ 0 & 0 & 0.0192 \end{bmatrix}. \tag{33}$$

When $\bar{\mathbf{M}}$ is increased over the above value, there are no further improvements of errors; in contrast, loud sounds from the robot joints were heard.

For only the TDCGE, the estimator gain matrix, $\mathbf{K_{GE}}$ are determined as

$$\mathbf{K_{GE}} = \begin{bmatrix} 50. & 0 & 0 \\ 0 & 45. & 0 \\ 0 & 0 & 71.5 \end{bmatrix}, \tag{34}$$

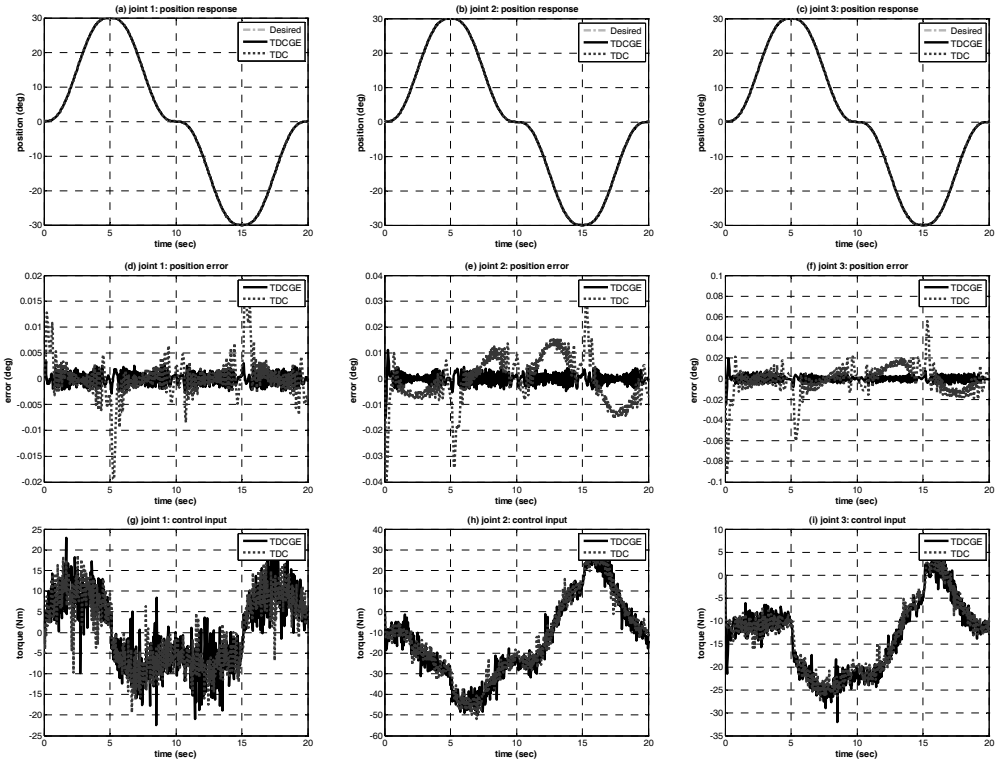


Fig. 10. Experimental Results of 3 DOF Robot Manipulator - TDC and TDCGE.

which is set with highest possible values without control chatter.

#### *4.2.2 Experimental results*

The experiment results are displayed in Fig. 10. The maximum tracking errors and the mean deviations of tracking errors are listed in Table 3 and 4, respectively.

Fig. 10(d), (e) and (f) clearly show that the TDC has large tracking errors due to Coulomb friction slightly after the instants when each joint of the controlled system crosses zero velocity as the case of 1 DOF linear motor. Coulomb friction belongs to a class of nonlinear friction having rapidly changing characteristics.

In comparison, however, the TDCGE reduces the tracking error vastly: the maximum error of joint 1 due to the TDCGE is about 18% of that of the TDC; the maximum error of joint 2 and 3 due to the TDCGE are about 35%. Fig. 10(g), (h) and (i) show that the TDCGE has a torque profile similar to that of the TDC and does not increase unwanted effects such as chattering. The experimental results confirm the effectiveness of the TDCGE against Coulomb friction, one of nonlinear friction, with similar level of input torque in the multi degree-of-freedom robot manipulator.

## 5. Conclusion

An enhanced control, called the TDCGE, is proposed for robot manipulators in this paper. The TDCGE is more robust than the TDC, because the TDE error is effectively cancelled out by the gradient estimator. The gradient estimator is a type of high pass filter for the TDE error. The TDCGE has a simple gain selection procedure as the TDC. Experiments with a 1 DOF linear motor and a 3 DOF spatial robot manipulator are carried out in order to verify the advantages of TDCGE, such as good robustness against nonlinear friction and simple design procedure.

At present, we are carrying out a profound study on the integral actions of the TDCGE and the relationship between the TDCGE and PID-based control. Upon the completion of the study, the result will be reported.

## Acknowledgment

This work was supported by Industrial Source Technology Development Programs (funded by the Ministry of Knowledge Economy (MKE, Korea). And we acknowledge discussion about the stability analysis with Dr. Maolin Kim.

## References

[1] K. Youcef-Toumi and O. Ito, A time delay controller design for systems with unknown dynamics. *ASME J. Dyn. Syst. Meas. Control,* 112 (1990) 133-142.

[2] K. Youcef-Toumi and S. T. Wu, Input/output linearization using time delay control. *ASME J. Dyn. Syst., Meas. Control,* 114 (1992) 10-19.

[3] T. C. Hsia, A new technique for robust control of servo systems. *IEEE Trans. Ind. Electron.,* 36 (1989) 1-7.

[4] T. C. Hsia and L. S. Gao, Robot manipulator control using

decentralized time-invariant time-delayed controller. *In: Proceedings of IEEE International Conference on Robotics and Automation,* (1990) 2070-2075.

[5] T. C. Hsia, T. A. Lasky and Z. Guo, Robust independent joint controller design for industrial robot manipulators. *IEEE Trans. Industrial Electronics,* 38 (1991) 21-25.

[6] P. H. Chang, D. S. Kim and K. C. Park, Robust force/ position control of a robot manipulator using time-delay control. *Control Engineering Practice,* 3 (1995) 1255-1264.

[7] S. Jung, T. C. Hsia and R. G. Bonitz, Force tracking impedance control of robot manipulators under unknown environment. *IEEE Trans. On Control Systems Technology,* 12 (2004) 474-483.

[8] J. Y. Park and P. H. Chang, Vibration control of a telescopic handler using time delay control and commandless input shaping technique. *Control Engineering Practice,* 12 (2004) 769-780.

[9] M. Jin and P. H. Chang, Simple robust technique using time delay estimation for the control and synchronization of Lorenz systems (2008), *Chaos, Solions and Fractals*, Article in Press.

[10] P. H. Chang and S. H. Park, On improving time-delay control under certain hard nonlinearities. *Mechatronics,* 13 (2003) 393-412.

[11] B. Armstrong, Friction: experimental determination, modeling and compensation. *In: Proceedings of IEEE International Conference on Robotics and Automation,* 3 (1988) 1422-1427.

[12] Tore Hägglund, A friction compensator for pneumatic control valves. *J. Process Control,* 12 (2002) 897-904.

[13] P. H. Chang and S. J. Lee, A straight-line motion tracking control of hydraulic excavator system. *Mechatronics,* 12 (2002) 119-138.

[14] J. H. Park and Y. M. Kim, Time-delay sliding mode control for a servo. *Trans. of ASME, J. Dyn. Sys. Meas. Contr.,* 121 (1999) 143-148.

[15] B. K. Kim, Task scheduling with feedback latency for real-time control systems. *In: Proceedings of International Conference on Real-time Computing System and Application* (1998) 37-41.

## Appendix

### *A.1 Stability analysis of TDCGE*

The globally uniformly ultimately boundedness of the overall systems with nonlinear friction is demonstrated.

If the Lyapunov function is considered as

$$\mathbf{V} = 0.5\tilde{\mathbf{E}}^{\mathbf{T}}\tilde{\mathbf{E}}\,, \tag{A.1}$$

where $\tilde{\mathbf{E}}$ denotes $\int \tilde{\boldsymbol{\varepsilon}} dt$, the time derivative of the Lyapunov function is then

$$\dot{\mathbf{V}} = -\tilde{\mathbf{E}}^{\mathbf{T}}\hat{\boldsymbol{\varepsilon}} + \tilde{\mathbf{E}}^{\mathbf{T}}\boldsymbol{\varepsilon}\,. \tag{A.2}$$

From $\hat{\boldsymbol{\varepsilon}} = \mathbf{K}_{\mathbf{GE}}\int \tilde{\boldsymbol{\varepsilon}} dt = \mathbf{K}_{\mathbf{GE}}\tilde{\mathbf{E}}$, Eq. (A.2) can be re-written as follows:

$$\dot{\mathbf{V}} = -\tilde{\mathbf{E}}^{\mathbf{T}}\mathbf{K}_{\mathbf{GE}}\tilde{\mathbf{E}} + \tilde{\mathbf{E}}^{\mathbf{T}}\boldsymbol{\varepsilon}\,. \tag{A.3}$$

It can be determined that

$$\text{if } \left|\tilde{\mathbf{E}}_i\right| > \mathbf{d}_i \text{ then } \dot{\mathbf{V}} < \mathbf{0}, \text{ where } \mathbf{d}_i = \left|\left\{\mathbf{K}_{\mathbf{GE}}^{-1}\boldsymbol{\varepsilon}\right\}_i\right|. \tag{A.4}$$

If $\boldsymbol{\varepsilon}$ is bounded, it can be concluded that $\tilde{\mathbf{E}}$ is globally uniformly ultimately bounded with the ultimate bound

$$\left|\tilde{\mathbf{E}}_i\right| \le \mathbf{d}_i\,. \tag{A.5}$$

This condition means the degradation of stability robustness due to the gradient estimator.

The boundedness of $\boldsymbol{\varepsilon}$ can be shown in the same manner of the stability proof shown in [4]. The closed-loop error dynamics of the proposed control (14) can be re-written as follows:

$$\begin{aligned} &\ddot{\mathbf{e}} + \mathbf{K}_{\mathbf{D}}\dot{\mathbf{e}} + \mathbf{K}_{\mathbf{P}}\mathbf{e} + \hat{\boldsymbol{\varepsilon}} = \boldsymbol{\varepsilon} \\ &\text{or } \mathbf{v} - \ddot{\boldsymbol{\theta}} = \boldsymbol{\varepsilon} \end{aligned}, \tag{A.6}$$

where $\mathbf{v} = \ddot{\boldsymbol{\theta}}_{\mathbf{d}} + \mathbf{K}_{\mathbf{D}}\left(\dot{\boldsymbol{\theta}}_d - \dot{\boldsymbol{\theta}}\right) + \mathbf{K}_{\mathbf{P}}\left(\boldsymbol{\theta}_{\mathbf{d}} - \boldsymbol{\theta}\right) + \hat{\boldsymbol{\varepsilon}}$ as (22).

Using (1) and (A.6) gives

$$\begin{aligned} \mathbf{M}(\boldsymbol{\theta})\boldsymbol{\varepsilon} &= \mathbf{M}(\boldsymbol{\theta})\left(\mathbf{v} - \ddot{\boldsymbol{\theta}}\right) \\ &= \mathbf{M}(\boldsymbol{\theta})\mathbf{v} + \mathbf{V}\left(\boldsymbol{\theta},\dot{\boldsymbol{\theta}}\right) + \mathbf{G}(\boldsymbol{\theta}) + \mathbf{F} + \mathbf{D} - \boldsymbol{\tau} \end{aligned}. \tag{A.7}$$

A combination of (8), (22) and (3) gives

$$\begin{aligned} \mathbf{M}(\boldsymbol{\theta})\boldsymbol{\varepsilon} &= \mathbf{M}(\boldsymbol{\theta})\mathbf{v} + \mathbf{V}\left(\boldsymbol{\theta},\dot{\boldsymbol{\theta}}\right) \\ &\quad + \mathbf{G}(\boldsymbol{\theta}) + \mathbf{F} + \mathbf{D} - \bar{\mathbf{M}}\mathbf{v} - \left(\boldsymbol{\theta},\dot{\boldsymbol{\theta}},\ddot{\boldsymbol{\theta}}\right)_{t-L}, \\ &= \left[\mathbf{M}(\boldsymbol{\theta}) - \bar{\mathbf{M}}\right]\mathbf{v} \\ &\quad - \left[\mathbf{M}(\boldsymbol{\theta})_{t-L} - \bar{\mathbf{M}}\right]\ddot{\boldsymbol{\theta}}_{t-L} + \boldsymbol{\Delta}, \\ &= \left[\mathbf{M}(\boldsymbol{\theta}) - \bar{\mathbf{M}}\right]\mathbf{v} - \left[\mathbf{M}(\boldsymbol{\theta}) - \bar{\mathbf{M}}\right]\ddot{\boldsymbol{\theta}}_{t-L} \\ &\quad - \left[\mathbf{M}(\boldsymbol{\theta})_{t-L} - \mathbf{M}(\boldsymbol{\theta})\right]\ddot{\boldsymbol{\theta}}_{t-L} + \boldsymbol{\Delta} \end{aligned} \tag{A.8}$$

where $\begin{aligned} \boldsymbol{\Delta} &= \mathbf{V}\left(\boldsymbol{\theta},\dot{\boldsymbol{\theta}}\right) + \mathbf{G}(\boldsymbol{\theta}) + \mathbf{F} + \mathbf{D} \\ &\quad - \mathbf{V}\left(\boldsymbol{\theta},\dot{\boldsymbol{\theta}}\right)_{t-L} - \mathbf{G}(\boldsymbol{\theta})_{t-L} - \mathbf{F}_{t-L} - \mathbf{D}_{t-L} \end{aligned}$.

As Coulomb friction and stiction in $\mathbf{F}$ are bounded, it is clear that $\boldsymbol{\Delta}$ is bounded for a sufficiently small $L$. Substituting $\ddot{\boldsymbol{\theta}}_{t-L} = \mathbf{v}_{t-L} - \boldsymbol{\varepsilon}_{t-L}$ from (A.6) into (A.8) yields

$$\begin{aligned} \mathbf{M}(\boldsymbol{\theta})\boldsymbol{\varepsilon} &= \left[\mathbf{M}(\boldsymbol{\theta}) - \bar{\mathbf{M}}\right]\mathbf{v} \\ &\quad + \left[\mathbf{M}(\boldsymbol{\theta}) - \bar{\mathbf{M}}\right]\left(\boldsymbol{\varepsilon}_{t-L} - \mathbf{v}_{t-L}\right) \\ &\quad - \left[\mathbf{M}(\boldsymbol{\theta})_{t-L} - \mathbf{M}(\boldsymbol{\theta})\right]\ddot{\boldsymbol{\theta}}_{t-L} + \boldsymbol{\Delta} \end{aligned} \tag{A.9}$$

$$\begin{aligned} \boldsymbol{\varepsilon} &= \left[\mathbf{I} - \mathbf{M}(\boldsymbol{\theta})^{-1}\bar{\mathbf{M}}\right]\boldsymbol{\varepsilon}_{t-L} \\ &\quad + \left[\mathbf{I} - \mathbf{M}(\boldsymbol{\theta})^{-1}\bar{\mathbf{M}}\right]\left(\mathbf{v} - \mathbf{v}_{t-L}\right) + \boldsymbol{\eta}_{\mathrm{l}} \end{aligned}, \tag{A.10}$$

where $\boldsymbol{\eta}_1 = \mathbf{M}(\boldsymbol{\theta})^{-1}\left\{\left[\mathbf{M}(\boldsymbol{\theta}) - \mathbf{M}(\boldsymbol{\theta})_{t-L}\right]\ddot{\boldsymbol{\theta}}_{t-L} + \boldsymbol{\Delta}\right\}$.

In the discrete-time domain, this can be represented as

$$\begin{aligned}\boldsymbol{\varepsilon}(k) = &\left[\mathbf{I} - \mathbf{M}(k)^{-1}\bar{\mathbf{M}}\right]\boldsymbol{\varepsilon}(k-1) \\ &+ \left[\mathbf{I} - \mathbf{M}(k)^{-1}\bar{\mathbf{M}}\right]\boldsymbol{\eta}_2(k) + \boldsymbol{\eta}_1(k)\end{aligned} \tag{A.11}$$

where $\boldsymbol{\eta}_1(k) = \mathbf{M}(k)^{-1}\left\{\left[\mathbf{M}(k) - \mathbf{M}(k-1)\right]\ddot{\boldsymbol{\theta}}(k-1) + \boldsymbol{\Delta}(k)\right\}$, and $\boldsymbol{\eta}_2(k) = \left[\mathbf{v}(k) - \mathbf{v}(k-1)\right]$.

In Eq. (A.11), $\boldsymbol{\eta}_1(k)$ and $\boldsymbol{\eta}_2(k)$, from the view point of $\boldsymbol{\varepsilon}(k)$, considered as forcing function, which are bounded for sufficiently small time-delay $L$. Clearly, (A.11) is a first-order discrete Eq. and asymptotically bounded if roots of $\left[\mathbf{I} - \mathbf{M}(k)^{-1}\bar{\mathbf{M}}\right]$ reside inside a unit circle. Appropriate values for $\bar{\mathbf{M}}$ should be selected to satisfy the stability.

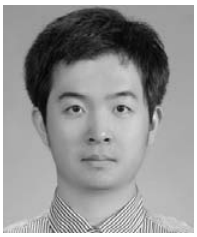

**Dong Ki Han** received the B.S. degree in mechanical engineering from Hanyang University, Seoul, Korea, in 2003, and the M.S. and Ph.D. degrees in mechanical engineering from Korea Advanced Institute of Science and Technology, Daejeon, Korea, in 2006 and 2010, respectively. His research interests include robust control of nonlinear systems, robot control, vibration control and pneumatic systems.

**Pyung Hun Chang** was born in Pusan, Korea, in 1951. He received the B.S. and M.S. degrees in mechanical engineering from Seoul National University, Seoul, Korea, in 1974 and 1977, respectively, and the Ph.D. degree in mechanical engineering from the Massachusetts Institute of Technology, Cambridge, in 1987. From 1984 to 1987, he was involved in a research project in the field of robotics as a Research Assistant in the Artificial Intelligence Laboratory, MIT. Since 1987, he has been a member of the faculty of the Department of Mechanical Engineering, Korea Advanced Institute of Science and Technology, Daejeon, Korea, where he is currently a Professor. His current research interests include robust impedance control of nonlinear plants as applied to robot manipulators and human impedance measuring, dynamic control of redundant manipulators, and the target-oriented design approach to rehabilitation robots and safety. Dr. Chang is a member of the American Society of Mechanical Engineers, the Korean Society of Mechanical Engineers, and the Korean Society for Precision Engineering.Busan, Korea.